EFFECTS OF TIN, ANTIMONY AND MOLYBDENUM IN Mn–W–O /$Ir_{1-x-y}Sn_xSb_yO_{2+0.5y}$/Ti ANODES FOR OXYGEN EVOLUTION IN SEAWATER ELECTROLYSIS

Jagadeesh Bhattarai
Central Department of Chemistry, Tribhuvan University, Kirtipur, Kathmandu, Nepal.

Abstract: An attempt was made to enhance the oxygen evolution efficiency in seawater electrolysis by the addition of tin, antimony and molybdenum to Mn–W oxide electrocatalysts prepared by anodic deposition on the intermediate $Ir_{1-x-y}Sn_xSb_yO_{2+0.5y}$/Ti electrode. $Ir_{1-x-y}Sn_xSb_yO_{2+0.5y}$/Ti supported nanocrystalline γ–MnO_2 type Mn–W–X–O(X=Sn,Sb,Mo) electrocatalysts with grain size of about 5-11 nm were tailored by anodic deposition. All the examined Mn–W–X(X=Sn,Sb,Mo)–O anodes showed the almost 100% oxygen evolution efficiency at 1000 $A.m^{-2}$ in 0.5 M NaCl solution of pH 1 at 25°C. They guaranteed the stable anode performance of about 99.75-99.85% oxygen evolution efficiencies for more than five months.

Keywords: Global warming; CO_2 recycling; Oxygen evolution anode; Seawater electrolysis; Hydrogen production electrode.

INTRODUCTION

The CO_2 emissions which induce global warming increase with the growth of the economic activity of the world. Since it is impossible to decrease the economic activity, it is also impossible to decrease the CO_2 emissions only by efforts for energy saving and by improvements of the energy efficiency. It has been reported that the energy consumption by a person in developed countries in 2005 was 5.9 times as high as that by a person in developing countries and the world energy consumption on the average during 18 years since 1990 resulted in 1.0193–fold increase every year[1]. This means a continuous increase in primary energy consumption results in continuous increase in carbon emissions. Such a huge carbon emissions resulting from complete exhaustion of fossil fuel reserves will induce intolerable global warming. Considering these facts, Professor Koji Hashimoto and his research groups at Tohoku University and Tohoku Institute of Technology have been proposed global CO_2 recycling project to prevent global warming and to supply abundant energy converted from solar energy[2-5].

Key materials necessary for the global CO_2 recycling project are anodes and cathodes for seawater electrolysis, and catalysts for CO_2 conversion into CH_2 from the reaction between CO_2 and H_2. Hashimoto and his co–workers are tailoring these key materials of anodes and cathodes for seawater electrolysis, and catalyst for CO_2 methanation. In general, seawater electrolysis is practically carried out for chlorine production in chlor alkali industry. Although the equilibrium potential of oxygen evolution is lower than that of chlorine evolution, the chlorine evolution is a simpler reaction than the oxygen evolution, and hence the formation of chlorine on the anode is generally unavoidable in seawater electrolysis. Nevertheless, for large–scale seawater electrolysis to produce the hydrogen gas at cathode for prevention of global warming, environmentally harmful chlorine release is not allowed. In this context, therefore, one of the most difficult subjects in tailoring key materials for the global CO_2 recycling was the anode for seawater electrolysis because, for CH_2 production a great quantity of chlorine emissions are not allowed, and hence the anode should evolve only oxygen with very high efficiency and durability even in seawater electrolysis at very high current density.

A variety of γ–MnO_2 type double or triple oxides for electrocatalysts of anodes were tailored by thermal decomposition[6,7] and anodic deposition[8-15] on the iridium dioxide (IrO_2)–coated titanium substrate, and these anodes showed about 90–100 % initial oxygen evolution efficiency in the electrolysis of 0.5 M NaCl solution at 1000 $A.m^{-2}$. These anodes were formed by two layers; the outer most layer is electrocatalysts of γ–MnO_2 type double or triple oxides and the intermediate oxide layer preventing the formation of insulating titanium oxide on the titanium substrate is generally IrO_2. However, in order to supply a future hydrogen demand in the world, the amount of iridium is not sufficient to manufacture the anodes for seawater electrolysis at all. Therefore, the alternative materials to IrO_2 those should have sufficient durability and conductivity at high potentials for anodic polarization, and the same rutile structure as TiO_2 are required. It has been reported that the γ–MnO_2 type triple oxide anodes on the intermediate layer of $Ir_{1-x-y}Sn_xSb_yO_{2+0.5y}$ / Ti electrode containing about 24% of IrO_2 with 10% of Sb_2O_5

showed about 99.7% oxygen evolution efficiency (OEE) after electrolysis for about 3400 h in 0.5 M NaCl of pH 1 at 1000 $A.m^{-2}$.[16-21] In this context, the present research work is focused to develop a more stable and efficient oxygen production Mn–W–X(X=Sn,Sb,Mo)–O anodes for seawater electrolysis. Particular attention was paid to the effect of the addition of Sn^{4+}, Sb^{5+} and Mo^{6+} ions to Mn–W–O/$Ir_{1-x-y}Sn_x$–$Sb_yO_{2+0.5y}$ / Ti anodes on the oxygen evolution efficiency.

MATERIALS AND METHODS

Punched titanium metal substrate was immersed in a 0.5 M HF solution for 5 minutes to remove air–formed oxide film, rinsed with de–ionized water and then subjected for surface roughening by etching in 11.5 M H_2SO_4 solution at 80°C until hydrogen evolution was ceased to enhance the anchor effect of the substrate on the electrocatalysts layer. Titanium sulfate on the titanium surface was removed by washing under tape water for about one hour. Then the treated–titanium metal was used as substrate for coating of the intermediate $Ir_{1-x-y}Sn_xSb_yO_{2+0.5y}$ layer. The $Ir_{1-x-y}Sn_xSb_yO_{2+0.5y}$ intermediate layer was prepared using coating solution which was prepared by mixing of 0.0240 M chloroiridic acid {$H_2IrCl_6.6H_2O$}, 0.0676 M tin chloride {$SnCl_4.5H_2O$} and 0.0084 M $SbCl_5$ butanolic solutions in which the sum of the metallic cations was kept at 0.1 M. The coating solution was used for coating on the treated–titanium substrate with a brush, dried at 80°C for 10 minutes, and then baked at 450°C for 10 minutes in air. This coating procedure was repeated three times so as to form the intermediate oxide layers of $Ir_{1-x-y}Sn_xSb_yO_{2+0.5y}$ on titanium substrate. This specimen was finally baked at 450°C for 1 h in air. The presence of the $Ir_{1-x-y}Sn_xSb_yO_{2+0.5y}$ layer is necessary to prevent the formation of insulating titanium oxide between electrocatalytically active substances and the titanium substrate during electrodeposition and electrolysis of seawater at high current density for a long time. This $Ir_{1-x-y}Sn_xSb_yO_{2+0.5y}$ coated titanium substrate was cut into 16 *x* 75 *x* 1 mm^3 as a suitable electrode, and a titanium wire was spot–welded to its edge. This is called the $Ir_{1-x-y}Sn_xSb_yO_{2+0.5y}$ /Ti electrode.

The $Ir_{1-x-y}Sn_xSb_yO_{2+0.5y}$ /Ti electrode was degreased by anodic polarization at 1000 $A.m^{-2}$ for 5 minutes in 10 M NaOH solution and then electroanalytically activated at 1000 $A.m^{-2}$ for 5 minutes in 1 M H_2SO_4 solution at room temperature. The Mn–Mo–X(X=Zn,Sn,W) oxide electrocatalysts for oxygen evolution were anodically deposited on the degreased and activated $Ir_{1-x-y}Sn_xSb_yO_{2+0.5y}$ /Ti electrode at 600 $A.m^{-2}$ in the solution containing 0.2 M $MnSO_4.5H_2O$ + 0.0045 M $Na_2WoO_4.2H_2O$ +{0.006M $SnCl_4.5H_2O$ or 0.003 M SbCl5 or/ and 0.003 M $Na_2MoO_4.2H_2O$} at pH –0.1 and 90°C for 90 minutes. The electrodeposition of the Mn–W–X(X=Sn,Sb,Mo) oxide electrocatalysts were carried out by exchanging electrolyte for every 30 minutes.

The performance of the Mn–W–X(X=Sn,Sb,Mo)–O/$Ir_{1-x-y}Sn_xSb_yO_{2+0.5y}$ /Ti anodes was examined by oxygen evolution efficiency and galvanostatic polarization measurements. The oxygen evolution efficiency was measured by electrolysis at a constant current density of 1000 $A.m^{-2}$ in 300 mL of 0.5 M NaCl solution of pH 1 (adjusted by adding concentrated hydrochloric acid) until the amount of charges of 300 coulombs was passed. The amount of oxygen evolved was determined as the difference between the total charge passed and the charge for chlorine formation during electrolysis as described elsewhere[7,13,22]. The amount of chlorine formed was analyzed by iodimetric titration of chlorine and hypochlorite.

Galvanostatic polarization measurement of the electrodeposited Mn–W–X (X=Sn,Sb,Mo)–O electrocatalysts on the $Ir_{1-x-y}Sn_xSb_yO_{2+0.5y}$ /Ti electrode was carried out in 0.5 M NaCl solution of pH 1 at 25°C. The ohmic drop was corrected using a current interruption method. The potential written in this paper is overpotential and is relative to Ag/AgCl reference electrode with saturated KCl solution.

The $Ir_{1-x-y}Sn_xSb_yO_{2+0.5y}$ /Ti electrodes and the anodically deposited Mn–Mo–X–O(X=Zn,Sn,W)/$Ir_{1-x-y}Sn_xSb_yO_{2+0.5y}$ / Ti anodes were characterized by X–ray diffraction (XRD) patterns with α–2θ mode using CuK_α radiation at a glancing angle α of 5°. The changes in the surface morphologies of the anodically deposited Mn–W–X(X=Sn,Sb,Mo)–O/$Ir_{1-x-y}Sn_xSb_yO_{2+0.5y}$ /Ti anodes were observed using confocal scanning laser microscope (CSLM). The laser source used was He–Ne having wavelength of 633 nm.

RESULTS AND DISCUSSION

Figure 1 shows X-ray diffraction patterns of the intermediate $Ir_{1-x-y}Sn_xSb_yO_{2+0.5y}$ layer on titanium substrate and the electrodeposited Mn–W–Mo–O/$Ir_{1-x-y}Sn_xSb_yO_{2+0.5y}$ /Ti anode. There are no separate peaks for IrO_2, SnO_2 and Sb_2O_5 at the XRD patterns of the intermediate $Ir_{1-x-y}Sn_xSb_yO_{2+0.5y}$ layer on titanium substrate, as shown in Fig. 1(a), indicating the formation of single–phase IrO_2–SnO_2–Sb_2O_5 layer. It is noteworthy to mention here that iridium, tin and antimony oxides on the titanium substrate were identified as IrO_2, SnO_2 and Sb_2O_5, respectively, from XPS analysis[16]. These results revealed that the intermediate $Ir_{1-x-y}Sn_xSb_yO_{2+0.5y}$ layer is composed of triple oxides of a rutile structure with fine grains instead of the mixture of oxides of iridium, tin and antimony. On the other hand, there are no separate peaks for manganese, tungsten and molybdenum oxides on the anodically deposited Mn–W–Mo–O/$Ir_{1-x-y}Sn_xSb_yO_{2+0.5y}$ /Ti anode. The XRD patterns of the anodically deposited Mn–W–Mo–O/$Ir_{1-x-y}Sn_xSb_yO_{2+0.5y}$ /Ti anode show only the reflections of γ–MnO_2 as shown in Fig. 1(b). Similarly, the XRD patterns of the all the other anodically deposited Mn–W–X(X=Sn,Sb,Mo)–O/ $Ir_{1-x-y}Sn_xSb_yO_{2+0.5y}$ /Ti anodes showed only the reflection of γ–MnO2. Furthermore, the apparent grain size of the anodically deposited Mn–Mo–X–O (X=Zr,Sn,W)/$Ir_{1-x-y}Sn_xSb_yO_{2+0.5y}$ /Ti anodes was estimated from full width at half maximum (FWHM) of the most intense XRD reflection by using the Scherrer's formula[23]. The estimated apparent grain size of the electrodeposited Mn–W–X–O(X=Sn,Sb,Mo) electrocatalysts was found to be in the ranges of 5–11 nm. These results revealed that the anodically deposited Mn–W–X–O(X=Sn,Sb,Mo)/$Ir_{1-x-y}Sn_xSb_yO_{2+0.5y}$ /Ti anodes consisted of a nanocrystalline γ–MnO_2–type triple/quadrate oxides consisting of Mn^{2+}, W^{6+}, Sn^{4+}, Sb^{5+} or Mo^{6+} ions.

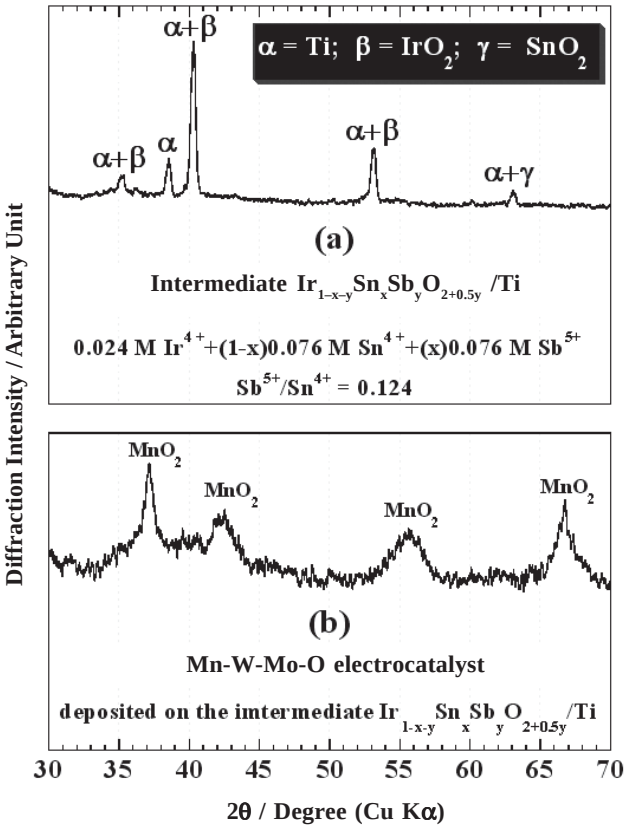

Figure 1: XRD patterns of the (a) $Ir_{1-x-y}Sn_xSb_yO_{2+0.5y}$ /Ti electrode and (b) anodically deposited Mn–W–Mo–O electrocatalyst on the $Ir_{1-x-y}Sn_xSb_yO_{2+0.5y}$ /Ti electrode.

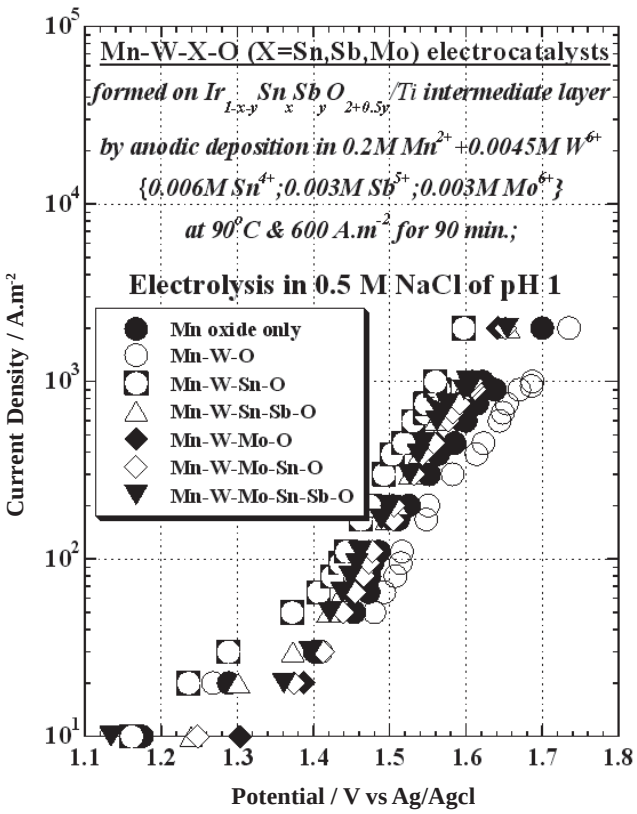

Figure 2: Galvanostatic polarization curves measured for Mn–W–X–O(X=Sn,Sb,Mo)/$Ir_{1-x-y}Sn_xSb_yO_{2+0.5y}$ /Ti anodes in 0.5 M NaCl of pH 1 at 25°C.

Figure 2 shows IR-corrected galvanostatic polarization curves measured in 0.5 M NaCl solution of pH 1 at 25°C for the anodically deposited Mn–W–X–O (X=Sn,Sb,Mo) electrocatalysts on the $Ir_{1-x-y}Sn_xSb_yO_{2+0.5y}$ /Ti electrode to study the effect of additional elements of tin, antimony and molybdenum in the Mn–W–O electrocatalysts. The anodically deposited Mn–W–Sn–O/$Ir_{1-x-y}Sn_xSb_yO_{2+0.5y}$ /Ti anode shows lowest oxygen overpotential at the current density of 1000 $A.m^{-2}$ among all the examined anodes in this study. Furthermore, the Mn–W–Sn–Sb–O/$Ir_{1-x-y}Sn_xSb_yO_{2+0.5y}$ /Ti, Mn–W–Mo–O/$Ir_{1-x-y}Sn_xSb_yO_{2+0.5y}$ /Ti, Mn–W–Mo–Sn–O/$Ir_{1-x-y}Sn_xSb_yO_{2+0.5y}$ /Ti and Mn–W–Mo–Sn–Sb–O/$Ir_{1-x-y}Sn_xSb_yO_{2+0.5y}$ /Ti anodes show almost same value of the oxygen overpotential at the current density of 1000 $A.m^{-2}$ and the oxygen overpotential of these anodes are lower than that of the MnO_2/$Ir_{1-x-y}Sn_xSb_yO_{2+0.5y}$ anode. These results revealed that the addition of tin, antimony and molybdenum in the Mn–W–based oxide electrocatalysts is more effective for high electronic conductivity of the Mn–W–X–O(X=Sn,Sb,Mo)/$Ir_{1-x-y}Sn_xSb_yO_{2+0.5y}$ /Ti anodes.

Figure 3 shows the effects of the additional elements on the Mn–W–X–O(X=Sn,Sb,Mo)/$Ir_{1-x-y}Sn_xSb_yO_{2+0.5y}$ /Ti anodes for oxygen overpotential at 1000 $A.m^{-2}$ and the initial oxygen evolution efficiency measured in 0.5 M NaCl solution of pH 1 at 25°C. The oxygen overpotentials at the current density of 1000 $A.m^{-2}$ for the Mn–W–Sn–Sb–O/$Ir_{1-x-y}Sn_xSb_yO_{2+0.5y}$ /Ti, Mn–W–Mo–O/$Ir_{1-x-y}Sn_xSb_yO_{2+0.5y}$ /Ti, Mn–W–Mo–Sn–O/$Ir_{1-x-y}Sn_xSb_yO_{2+0.5y}$ /Ti and Mn–W–Mo–Sn–Sb–O/$Ir_{1-x-y}Sn_xSb_yO_{2+0.5y}$ /Ti anodes are almost same (that is, about in 1.60 V vs Ag/AgCl) and the overpotential values of these anodes are lower than that of the MnO_2/$Ir_{1-x-y}Sn_xSb_yO_{2+0.5y}$ /Ti and are higher than that of the Mn–W–Sn–O/$Ir_{1-x-y}Sn_xSb_yO_{2+0.5y}$ /Ti anode as shown in Fig.3. It is noteworthy to mention here that the oxygen overpotential value of 1.60 V vs Ag/AgCl at 1000 $A.m^{-2}$ observed in the present study is almost same value as reported for the anodically deposited Mn–X–Y–O(X=W,Mo &Y=Sn)/IrO_2/Ti anodes[8,9,12,14]. However, the amount of iridium content in the intermediate oxide layer of the $Ir_{1-x-y}Sn_xSb_yO_{2+0.5y}$ /Ti electrode is only about 1/22 of the IrO_2/Ti electrodes. These results revealed that the addition of SnO_2 with small amount of Sb_2O_5 to the intermediate layer of the Mn–X–Y–O(X=W,Mo & Y=Sn,Sb)/$Ir_{1-x-y}Sn_xSb_yO_{2+0.5y}$ /Ti anodes is effective to decrease the use of IrO_2 to about 1/22, maintaining high electronic conductivity of the intermediate $Ir_{1-x-y}Sn_xSb_yO_{2+0.5y}$ layer on titanium substrate. On the other hand, the additions of tin, antimony and molybdenum on the Mn–W–O/$Ir_{1-x-y}Sn_xSb_yO_{2+0.5y}$ /Ti anodes show high activity of the oxygen evolution efficiency of about 98–99% or more in seawater electrolysis. In particular, the initial oxygen evolution efficiency of the Mn–W–Mo–O/$Ir_{1-x-y}Sn_xSb_yO_{2+0.5y}$ /Ti, Mn–W–Mo–Sn–O/$Ir_{1-x-y}Sn_xSb_yO_{2+0.5y}$ /Ti and Mn–W–Mo–Sn–Sb–O/$Ir_{1-x-y}Sn_xSb_yO_{2+0.5y}$ /Ti anodes show about 99% oxygen evolution efficiency in 0.5 M NaCl solution of pH 1 at 25°C (Fig.3).

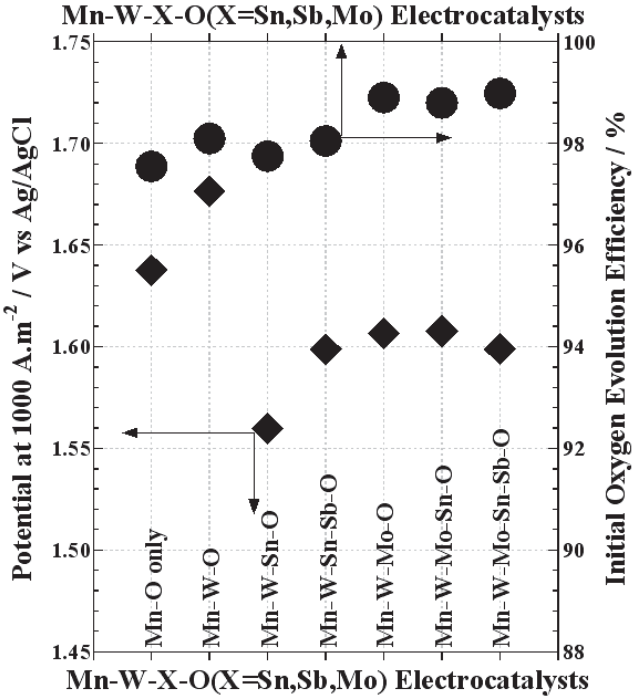

Figure 3: Changes in the oxygen overpotential and initial oxygen evolution efficiency of the Mn–W–X–O(X=Sn,Sb,Mo)/$Ir_{1-x-y}Sn_xSb_yO_{2+0.5y}$/Ti anodes in 0.5 M NaCl of pH 1 at the current density of 1000 A.m^{-2}.

The durability test on the Mn–W–based oxide electrodes was carried out. Figure 4 shows the durability result on the Mn–W–X–O(X=Sn,Sb,Mo)/$Ir_{1-x-y}Sn_xSb_yO_{2+0.5y}$/Ti anodes in 0.5 M NaCl solution of pH 1 at 25°C. The initial oxygen

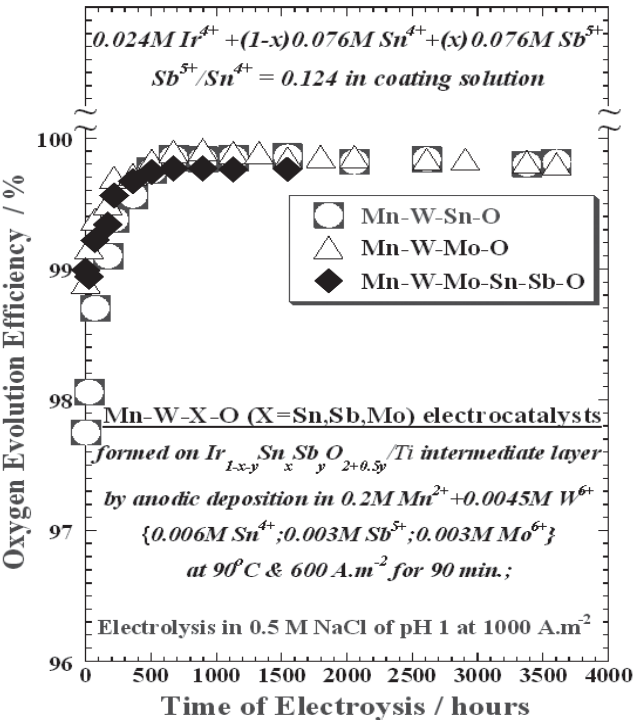

Figure 4: Changes in the oxygen evolution efficiency of the Mn–W–X (X=Sn,Sb,Mo)–O electrocatalysts deposited on the $Ir_{1-x-y}Sn_xSb_yO_{2+0.5y}$ intermediate layer on titanium substrate in 0.5 M NaCl of pH 1 at the current density of 1000 A.m^{-2}, as a function of electrolysis time.

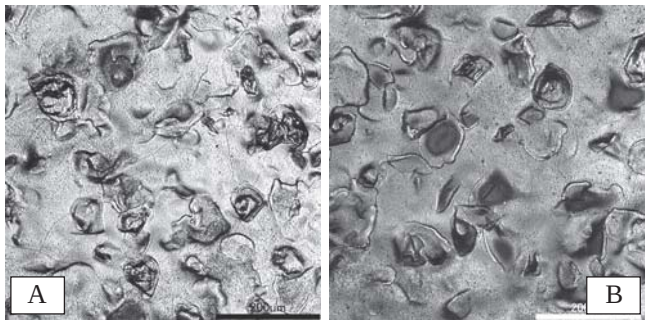

Figure 5: Changes in the surface morphology of the Mn–W–Mo–O electrocatalyst deposited on the $Ir_{1-x-y}Sn_xSb_yO_{2+0.5y}$/Ti electrode (a) before and (b) after electrolysis for 1545 h in 0.5 M NaCl solution of pH 1 at 1000 A.m^{-2}.

evolution efficiency of the Mn–W–Sn–O electrocatalyst is about 97.75 %, whereas that of the Mn–W–Mo–O electrocatalyst is about 99%. However, both of these electrocatalysts show almost 100% oxygen evolution efficiency and exhibit better durability for long time electrolysis of 0.5 M NaCl at pH 1. Consequently, the addition of molybdenum is effective in improving the initial oxygen evolution, but tin addition to Mn–W–O electrocatalyst is more active for oxygen evolution reaction with long–term electrolysis. All the three examined anodes showed about 99.75 to 99.85 % oxygen evolution efficiency in the electrolysis of 0.5 M NaCl of pH 1 at 25°C and the oxygen evolution efficiency is independent of the electrolysis time for about 3600 hours. The Mn–W–Sn–O/$Ir_{1-x-y}Sn_xSb_yO_{2+0.5y}$/Ti and Mn–W–Mo–O/$Ir_{1-x-y}Sn_xSb_yO_{2+0.5y}$/Ti anodes show slightly higher oxygen evolution efficiency of about 99.85% than that of the Mn–W–Mo–Sn–Sb–O/$Ir_{1-x-y}Sn_xSb_yO_{2+0.5y}$/Ti anode.

Figures 5 and 6 show the changes of the surface morphologies of the Mn–W–Mo–O/$Ir_{1-x-y}Sn_xSb_yO_{2+0.5y}$/Ti and Mn–W–Mo–Sn–Sb–O/$Ir_{1-x-y}Sn_xSb_yO_{2+0.5y}$/Ti anodes, respectively, before and after electrolysis in 0.5 M NaCl solution of pH 1 at the current density of 1000 A.m^{-2} for about 1545 hours. In both anodes, numbers of cracks and pores on the surface of the anodically deposited anodes were decreased to form a smooth surface after electrolysis for 1545 hours in 0.5 M NaCl solution. This revealed that the filling of the cracks by the beneficial ions (Mn^{2+}, W^{6+}, Mo^{6+}, Sn^{4+} or Sb^{5+}) presence in the electrocatalysts was clearly observed after electrolysis of the anodes for hundreds of hours. In accordance of the

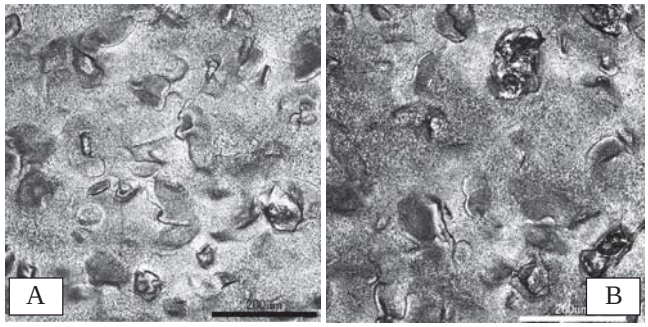

Figure 6: Changes in the surface morphology of the Mn–W–Mo–Sn–Sb–O electrocatalyst deposited on the $Ir_{1-x-y}Sn_xSb_yO_{2+0.5y}$/Ti electrode (a) before and (b) after electrolysis for 1545 h in 0.5 M NaCl solution of pH 1 at 1000 A.m^{-2}.

changes in the surface morphologies, the durability of the oxygen evolution efficiency of these two anodes increased with increasing the electrolysis times and became steady state after electrolysis for about 500 hours as shown in Fig. 4.

CONCLUSIONS

Successfully tailored new types of anodically deposited nanocrystalline Mn–W–Sn–O, Mn–W–Mo–O, Mn–W–Mo–Sn–O and Mn–W–Mo–Sn–Sb–O electrocatalysts on the intermediate $Ir_{1-x-y}Sn_xSb_yO_{2+0.5y}$ layer on titanium substrate for the production of hydrogen gas from seawater electrolysis with forming less than 0.25% of the environmentally harmful chlorine. The high oxygen evolution efficiency of these oxide electrocatalysts maintained during prolonged electrolysis, and even after the electrolysis for five or more months, the Mn–W–X–O(X=Sn,Sb,Mo)/$Ir_{1-x-y}Sn_xSb_yO_{2+0.5y}$ /Ti anodes showed an oxygen evolution efficiency of about 99.75–99.85%. The addition of tin, antimony and molybdenum in Mn–W–O electrocatalyst is effective to maintain the high electronic conductivity and high activity of oxygen evolution of the anodes for seawater electrolysis at pH 1 at high current density of 1000 $A.m^{-2}$.

ACKNOWLEDGEMENTS

The author would like to express his sincere gratitude to Emeritus Professor Dr. Koji Hashimoto and Dr. Zenta Kato of Tohoku Institute of Technology, Sendai, Japan for providing the research facilities of coating, XRD measurements and an opportunity to visit Tohoku Institute of Technology, Japan as a Visiting Research Fellow supported by Diaki Atka Engineering Co. Ltd., Japan. Sincere thanks to Dr. Himendra Jha, Post–doctoral Fellow at the LIMSA, Hokkaido University, Japan for his kind helps for taking the CSLM images.

REFERENCES

1. Hashimoto, K., Kato, Z., Kumagai, N. and Izumiya, K. 2009. *Journal of Physics: Conference Series.* **144**: 1–6.
2. K. Hashimoto, K. 1994. *Materials Science and Engineering*. **A179/A180**: 27–30.
3. Hashimoto, K. 1994. *Transactions of Materials Research Society of Japan*. **18A:** 35–40.
4. Hashimoto, K., Yamasaki, M., Fujimura, K., Matsui, T., Izumiya, K., Komori, M., El–Moneium, A. A., Akiyama, E., Habazaki, H., Kumagai, N., Kawashima, A. and Asami, K. 1999. *Materials Science and Engineering*. **A267:** 200–206.
5. Hashimoto, K., Habazaki, H., Yamazaki, M., Meguro, S., Sasaki, T., Katagiri, H., Matsui, T., Fujimura, K., Izumiya, K., Kumagai, N. and Akiyama, E. 2001. *Materials Science and Engineering*, **A304–306:** 88–96.
6. Izumiya, K., Akiyama, E., Habazaki, H., Kawashima, A., Asami, K. and Hashimoto, K. 1997. *Journal of Applied Electrochemistry*. **27:** 1362–1368.
7. Izumiya, K., Akiyama, E., Habazaki, H., Kumagai, N., Kawashima, A. and Hashimoto. 1997. *Materials Transactions, Journal of Institute of Metals.* **38:** 899–905.
8. Izumiya, K., Akiyama, E., Habazaki, H., Kumagai, N., Kawashima, A. and Hashimoto. 1998. *Electrochimica Acta*. **43:** 3303–3312.
9. Fujimura, K., Izumiya, K., Kawashima, A., Akiyama, E., Habazaki, H., Kumagai, N. and Hashimoto, K. 1999. *Journal of Applied Electrochemistry*. **29:** 765–771.
10. Fujimura, K., Matsui, T., Izumiya, K., Kumagai, N., Akiyama, E., Habazaki, H., Kawashima, A., Asami, K. and Hashimoto, K. 1999. *Materials Science and Engineering*. **A267:** 254–259.
11. Fujimura, K., Matsui, T., Habazaki, H., Kawashima, A., Kumagai, N. and Hashimoto, K. 2000. *Electrochimica Acta*. **45:** 2297–2303.
12. Habazaki, H., Mastui, T., Kawashima, A., Asami, K., Kumagai, N. and Hashimoto, K. 2001. *Scripta Materials*. **44:** 1659–1662.
13. Abdel Ghany, N. A., Kumagai, N., Meguro, S., Asami, K. and Hashimoto, K. 2002. *Electrochimica Acta*. **48:** 21–28.
14. El–Moneim, A. A., Kumagai, N., Asami, K. and Hashimoto, K. 2006. in *Corrosion and Electrochemistry of Advanced Materials in Honor of Koji Hashimoto* (Eds; S. Fujimoto, H. Habazaki, E. Akiyama and B. MacDougall), ECS Transactions. The Electrochemical Society, Pennington, NJ. **1(4):** 491–498.
15. Kato, Z., Kumagai, N., Asami, K. and Hashimoto, K. 2006. in *Corrosion and Electrochemistry of Advanced Materials in Honor of Koji Hashimoto* (Eds; S. Fujimoto, H. Habazaki, E. Akiyama and B. MacDougall), ECS Transactions. The Electrochemical Society, Pennington, NJ. **1(4):** 499–507.
16. Bhattarai, J., Shinomiya, H., Kato, Z., Izumiya, K., Kumagai, N. and Hashimoto, K. 2007. in *Proceeding 54th Japan Conference on Materials and Environments*, Japan Society of Corrosion Engineers (JSCE), Hiroshima, Japan. **C–207:** 345–348.
17. Kato, Z., Bhattarai, J., Izumiya, K., Kumagai, N. and Hashimoto, K. 2008. The improvement of the intermediate layer by substitution of iridium with tin in Mn–Mo–Sn triple oxide/IrO_2/Ti anodes for oxygen evolution in seawater electrolysis. in *Abstract book of 214th Electrochemical Society Meeting*, **Abstract No.1632**. The Electrochemical Society, Pennington, NJ.
18. Bhattarai, J. 2008/2009. *Journal of Nepal Chemical Society.* **23:** 2–32.
19. Bhattarai, J. 2008/2009. *Journal of Nepal Chemical Society.* **23:** 54–64.
20. Kato, Z., Bhattarai, J., Izumiya, K., Kumagai, N. and Hashimoto, K. 2009. The improvement of the intermediate layer by formation of tin–iridium dioxide in oxygen evolution anodes for seawater electrolysis. in *Abstract book of 216th Electrochemical Society Meeting*, **Abstract No. 1942**. The Electrochemical Society, Pennington, NJ.
21. El-Moneim, A. A., Bhattarai, J., Kato, Z., Izumiya, K., Kumagai, N. and Hashimoto, K. 2010. Mn-Mo-Sn oxide anodes for oxygen evolution in seawater electrolysis for hydrogen production. in *Oxide Films* (Eds; P. Marcus, S. Fujimoto and H. Terryn), ECS Transactions. The Electrochemical Society, Pennington, NJ. **25(40):** 127–137.
22. Kumagai, N., Samata, Y., Kawashima, A., Asami, K. and Hashimoto, K. 1987. *Journal of Applied Electrochemistry*. **17:** 347.
23. Cullity, B. D. 1977. in *Elements of X-ray Diffraction*, 2nd edition, Addison–Wesley Publ. Co, Inc., Pp.101.

***